


## Enhancing qubit readout with Bayesian learning

F. Cosco<sup>1,\*</sup> and N. Lo Gullo<sup>2,3,†</sup>

<sup>1</sup>*Quantum Algorithms and Software, VTT Technical Research Centre of Finland Ltd, Tietotie 3, 02150 Espoo, Finland*

<sup>2</sup>*Dipartimento di Fisica, Università della Calabria, Arcavacata di Rende, I-87036 Cosenza, Italy*

<sup>3</sup>*INFN - Gruppo Collegato di Cosenza, Arcavacata di Rende, I-87036 Cosenza, Italy*

 (Received 28 February 2023; accepted 28 November 2023; published 22 December 2023)

We introduce an efficient and accurate readout measurement scheme for single and multiqubit states. Our method uses Bayesian inference to build an assignment probability distribution for each qubit state based on a reference characterization of the detector response functions. This allows us to account for system imperfections and thermal noise within the assignment of the computational basis. We benchmark our protocol on a quantum device with five superconducting qubits, testing initial state preparation for single- and two-qubit states and an application of the Bernstein-Vazirani algorithm executed on five qubits. Our method shows a substantial reduction of the readout error and promises advantages for near-term and future quantum devices.

DOI: [10.1103/PhysRevA.108.L060402](https://doi.org/10.1103/PhysRevA.108.L060402)

**Introduction.** The promises of quantum computing as a revolutionary technology are being challenged by severe technological limitations in the current hardware. The noise level in the single- and two-qubit gates is undoubtedly one such factor [1], if not the most important one at the moment.

On the one hand, this prevents the building of fault-tolerant quantum computers and makes the current noisy intermediate-scale quantum (NISQ) processing units of limited use, especially when compared with classical (super)computers. On the other hand, these limitations are fostering the emergence of new research aiming at exploiting these devices as they are [2–4]. Possible solutions range from improving the design of quantum processing units (QPUs) [5,6] and noise-resilient qubit registers [7–10] to improving the control electronics, from increasing manufacturing quality [11] to creating algorithms and software to optimize the data pre- and postprocessing or recurring to quantum optimal control theory [12–15].

Quantum error mitigation is the general framework grouping all techniques that aim to improve the performances of NISQ processing units [16–20], typically by postprocessing the data of the quantum computation to decrease noise impact [21,22], but not without some fundamental limitation [23,24].

In a quantum processor, errors arise at all different stages of computation alike in a classical one: (i) when loading data (state preparation), (ii) during data processing (circuit execution), and (iii) at the moment of the readout (measurement). Most of the focus has been on mitigating errors at the level of the quantum circuit execution, e.g., zero noise extrapolation [25–29]. However, several recent works have focused on improving the readout fidelity [30–42]. These approaches include a series of techniques aiming at improving the pulse protocol before the measurement [43], finding the optimal

readout time [44] for the wanted fidelity of the discrimination or the postprocessing of the counts [45]. Methods which manipulate the outcomes statistics, with the inversion of the confusion matrix, may attain the intended results but can yield nonphysical values, an issue commonly addressed by incorporating a convex optimizer in the mitigation pipeline [46]. Additionally, the scalability of matrix inversion can become challenging when dealing with higher dimensions. Some other proposals to improve the discrimination between the two states which are gaining attention are based on machine-learning-based techniques [21], either in postprocessing [47] or during the readout protocol [48–50].

In this work, we introduce a statistical readout framework based on Bayesian inference, inspired by successful application of Bayesian inference in quantum metrology and sensing [51,52] or parameter estimation for quantum circuits and states [53–60]. Our Bayesian learning readout (BaLeRO) relies upon two steps: (i) characterization of the readout device to build the detector response functions, akin to detector tomography [45,61], and (ii) postprocessing data obtained from the circuit execution using a Bayesian update rule and

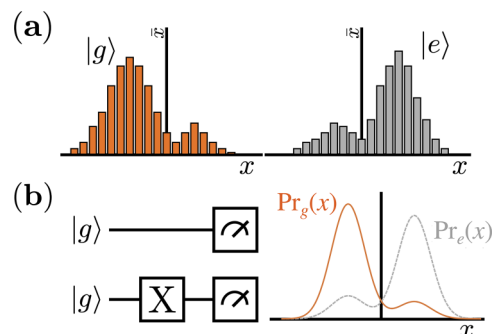


FIG. 1. (a) Typical qubit-state-dependent response functions. (b) Sketch of the characterization step: circuits and fit of the response functions  $\text{Pr}_g(x)$  and  $\text{Pr}_e(x)$ .

\*francesco.cosco@vtt.fi

†nicolino.logullo@unical.it

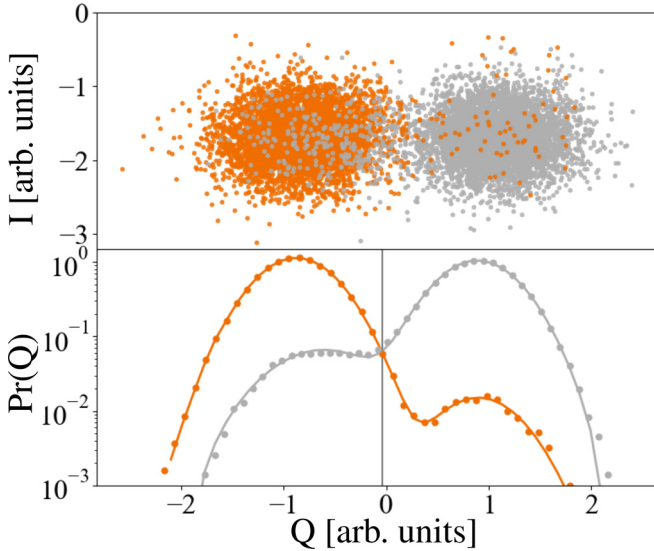


FIG. 2. (Top) Measurement clouds in IQ plane. (Bottom) Projected histograms and fitted response functions of IBM Quito Q4.

the functions obtained from the first step. Moreover, the postprocessing algorithm's input is the raw data from the detector (e.g., quantum analyzer), and the output is some probability distribution for the occupation of the computational basis (e.g., for a single qubit  $|0\rangle$  and  $|1\rangle$ ). Crucially, this approach is not a single-shot discriminator but leverages all measurement data to reconstruct the system density matrix. Our method avoids nonphysical outcomes, offering stability when extending to multiqubit scenarios, avoiding posterior optimization and noise matrix inversion altogether with an iterative approach. Our Bayesian readout constructs a probability distribution for qubit populations consistent with the measured data, regardless of the system dimension. In what follows, we first introduce the single-qubit framework as a foundational step. Then, we show how to extend the methodology to operate in higher dimensions with a larger number of qubits without suffering the issues arising in other methods based on the inversion of the noise matrix.

We show that our algorithm can improve the results obtained on actual QPUs for several quantum circuits and algorithms. Although we primarily focus on superconducting qubit devices, the approach could be applied to other platforms which allow for the reconstruction of the readout device response functions.

*Embrace the noise.* A qubit is encoded in a quantum system with at least two distinguishable states, say,  $|g\rangle$  (ground) and  $|e\rangle$  (excited). The readout procedure aims at assigning 0 or 1, depending on which of those states the qubit is in during the measurement. However, detection is not perfect. Instead of getting two distinguished and sharp signals depending on the qubit's two possible states, a detector's typical response function is similar to the one in Fig. 1(a). The 0 or 1 assignment is done through a separatrix which discriminates the state after each measurement. The separatrix is calibrated beforehand and might be either a curve in a two-dimensional space, like the IQ-plane of Fig. 2 (top) for superconducting qubits [62], or a threshold in a projected space as in Fig. 2 (bottom). Hence, the standard readout method assigns either a 0 or 1 based

on the relative position of the physical value with respect to the separatrix for each individual measurement. Once all individual measurements are completed, they are aggregated to yield the final count statistics. This approach is prone to a significant error because of the overlap between the two signals, which is caused by all possible noise sources.

To mitigate these issues, we develop a radically different approach to the problem, which *embeds* the base readout noise into the *assignment* process. We achieve the goal in two steps: (i) characterization of the detector and (ii) postprocessing of the data collected after the execution of a generic quantum circuit through a Bayesian-like update rule. We characterize the detector by performing two simple experiments: reset of the qubit and measurement and flip of the qubit to the excited state and measurement. The two processes are depicted as quantum circuits in Fig. 1(b) (left). We repeat these experiments and collect enough data to build two probability distributions  $\Pr_g(x)$  and  $\Pr_e(x)$ . They can be interpreted as the probability distributions of measuring the physical value  $x$  (e.g., a voltage) when the qubit is in the ground or excited state. We construct model fits for these distributions as shown in Fig. 1(b) (right) and in Fig. 2 using bimodal Gaussian distributions. We observe a finite interval of values of  $x$  for which the two distributions overlap. For these detector outcomes, assessing the qubit's state and assigning the value 0 or 1 unambiguously is impossible. This is the primary source of error in the separatrix-based assignment, *regardless* of the error's microscopic source. The second step is now to process the outcomes of any quantum circuit. To formalize our approach, we define two events: (1) the detector returns  $x$  when measuring the state of the qubit and (2) the qubit's density matrix populations are  $\{\rho_g, \rho_e\}$ , i.e., the probability that a measurement performed in the computational basis will find the system in  $|0\rangle$  or  $|1\rangle$ , respectively. These two events are dependent, and we leverage their statistical correlation to process the readout outcomes. Using the model distributions, we define the conditional probability for the detector measuring  $x$  given that the qubit's state is characterized by the pair  $\{\rho_g, \rho_e\}$ :

$$\Pr(x|\{\rho_g, \rho_e\}) = \frac{\rho_g \Pr_g(x) + \rho_e \Pr_e(x)}{\rho_g + \rho_e}. \quad (1)$$

Likewise, from Bayes' theorem, we can formally write the conditional probability for the qubit's state populations given a measured value of  $x$ :

$$\Pr(\{\rho_g, \rho_e\}|x) = \frac{\Pr(x|\{\rho_g, \rho_e\})\Pr(\{\rho_g, \rho_e\})}{\Pr(x)}. \quad (2)$$

Contrarily to the common approach, our algorithm leverages Eq. (1) and the full set of the detector's measurement outcomes  $\mathbf{x} = x^{(1)}, \dots, x^{(N_{\text{shots}})}$  through a Bayesian update rule:

$$\begin{aligned} \Pr(\{\rho_g, \rho_e\}|x^{(n)}) &\propto \Pr(x^{(n)}|\{\rho_g, \rho_e\})\Pr(\{\rho_g, \rho_e\}) \\ &= [\rho_g \Pr_g(x^{(n)}) + \rho_e \Pr_e(x^{(n)})]\Pr(\{\rho_g, \rho_e\}) \\ &\approx [\rho_g \Pr_g(x^{(n)}) + \rho_e \Pr_e(x^{(n)})]\Pr(\{\rho_g, \rho_e\}|x^{(n-1)}), \end{aligned} \quad (3)$$

where  $\Pr(\{\rho_g, \rho_e\})$  is the prior probability distribution and it is updated after each iteration step with the posterior probability distribution  $\Pr(\{\rho_g, \rho_e\}|x^{(n-1)})$  at the previous step.

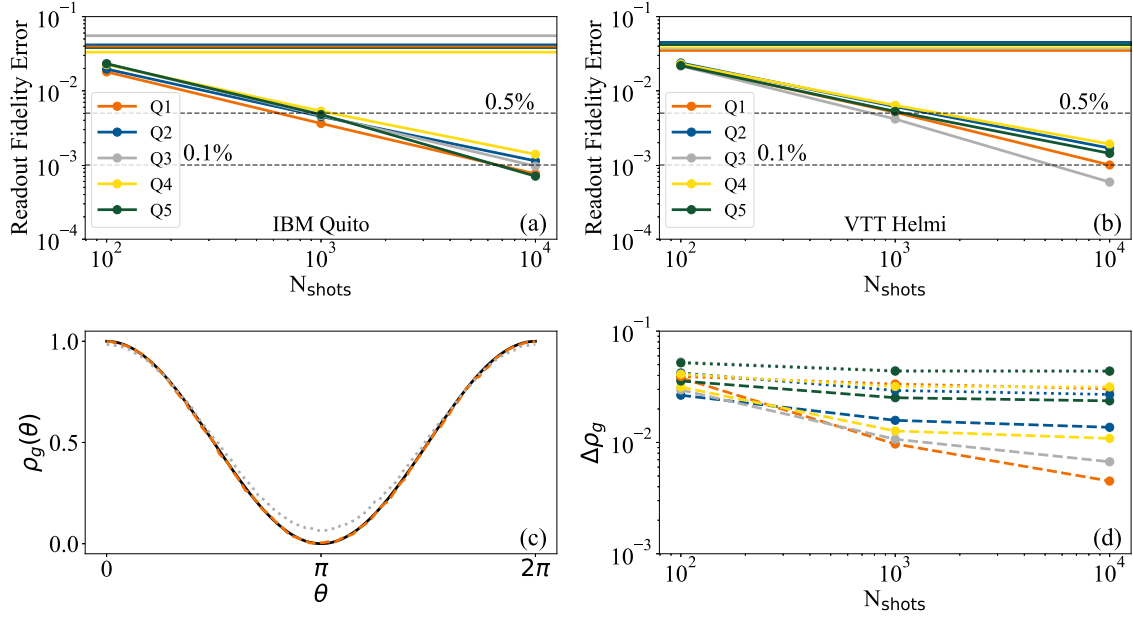


FIG. 3. (a) and (b) Readout fidelity error using BaLeRO as a function of the number of shots for each qubit on IBM Quito and VTT Helmi. The horizontal lines correspond to the errors reported by the service provider [63] (in the appropriate color scheme for each qubit). (c) Ground-state population of Q1 (IBM Quito) after applying a  $R_y(\theta)$  gate. The solid black line corresponds to the ideal population, the dotted gray one to the counts estimate, and the dashed orange to the BaLeRO estimate with  $10^4$  shots. (d) Average ground-state population error,  $\Delta\rho_g = 1/(2\pi) \int d\theta |\cos(\theta/2)^2 - \rho_g(\theta)|$ , as a function of the number of shots for each qubit (IBM Quito). Dotted and dashed lines refer to the counts and BaLeRO estimates, respectively [color scheme as in (a)].

When assuming no prior knowledge about the system state, we start the iteration with a uniform probability distribution  $\Pr(\{\rho_g, \rho_e\} | x^{(0)})$ .

Within this framework, we work with a probability distribution defined on the plane  $\{\rho_g, \rho_e\}$ , in the region which satisfies  $\rho_g + \rho_e = 1$ . The result is the probability distribution  $\Pr(\{\rho_g, \rho_e\} | x^{(N_{\text{shots}})})$ , which represents the probability distribution for the qubit's state populations coherent with the collected raw measurement data. With this we can compute the average value of *any* single qubit operator projected onto the computational basis or simply recover an estimate for the qubit populations via integration, i.e.,  $\rho_{g/e}^{\text{est}} = \int d\rho_g d\rho_e \rho_{g/e} \Pr(\{\rho_g, \rho_e\} | x^{(N_{\text{shots}})})$ .

The method is not limited to single-qubit readout, but it can be applied to any multiqubit system following similar steps. Given a system of  $N_q$  qubits, and  $N_q$  independent detectors registering the set of measurement outcomes  $\mathbf{x} = x_1, \dots, x_{N_q}$  for each shot, the multidimensional response function depends now on the population of each multiqubit state and is written as

$$\Pr(\mathbf{x} | \rho \equiv \rho_0, \dots, \rho_{2^{N_q}-1}) = \sum_i \rho_i \Pr_i(\mathbf{x}), \quad (4)$$

where  $\rho_i$  is the population of the  $i$ th state, e.g.,  $|\rho_0\rangle = |0\dots 0\rangle$ ,  $|\rho_1\rangle = |0\dots 1\rangle$  up to  $|\rho_{2^{N_q}-1}\rangle = |1\dots 1\rangle$ , and  $\Pr_0(\mathbf{x}) = \Pr_g(x_1)\Pr_g(x_2)\dots\Pr_g(x_{N_q})$ ,  $\Pr_1(\mathbf{x}) = \Pr_g(x_1)\Pr_g(x_2)\dots\Pr_e(x_{N_q})$ , and so forth. The posterior probability distribution for the population of each state can be then reconstructed in a sequence of single-shot measurements following the Bayes theorem as

previously introduced,

$$\Pr(\rho | \mathbf{x}^{(n)}) \propto \sum_i \rho_i \Pr_i(\mathbf{x}^{(n)}) \Pr(\rho | \mathbf{x}^{(n-1)}), \quad (5)$$

within the parameters space which satisfies  $\sum_i \rho_i = 1$ . It is worth mentioning that our approach shares some similarities with the iterative Bayesian unfolding, which is a form of regularized matrix inversion applied to the response matrix [64,65]. Here, however, we bypass the faulty state-assignment step and work on the continuous space of the physical measurement.

*Improvement of readout fidelities.* We test our readout scheme on two five-qubit quantum computers, the IBM Quito and the VTT Helmi (QPU from IQM). We start by reconstructing the reference response functions by running the circuits depicted in Fig. 1(b) for  $N_{\text{shots}} = 10^5$ . A typical outcome is the one displayed in Fig. 2 (top panel) where each measurement is represented by a dot in the I-Q plane. The clouds are then often rotated and projected onto one of the axes to obtain the distributions shown in Fig. 2 (bottom panel). We use these histograms to fit the probability distributions  $\Pr_g(x)$  and  $\Pr_e(x)$  using bimodal Gaussians. We repeat the characterization procedure for each qubit on the device and then use the obtained response functions to analyze the assignment fidelity in subsequent experiments. In Figs. 3(a) and 3(b), we show the average error related to the readout fidelity for each qubit as a function of the number of shots using BaLeRO. Interestingly, we are able to attain a readout error below 0.5% already below  $10^4$  shots, significantly improving the readout error reported by the service provider, which is typically of the order of  $\lesssim 5\%$ . Strikingly, with our protocol, the readout fidelity improves with an increasing number of

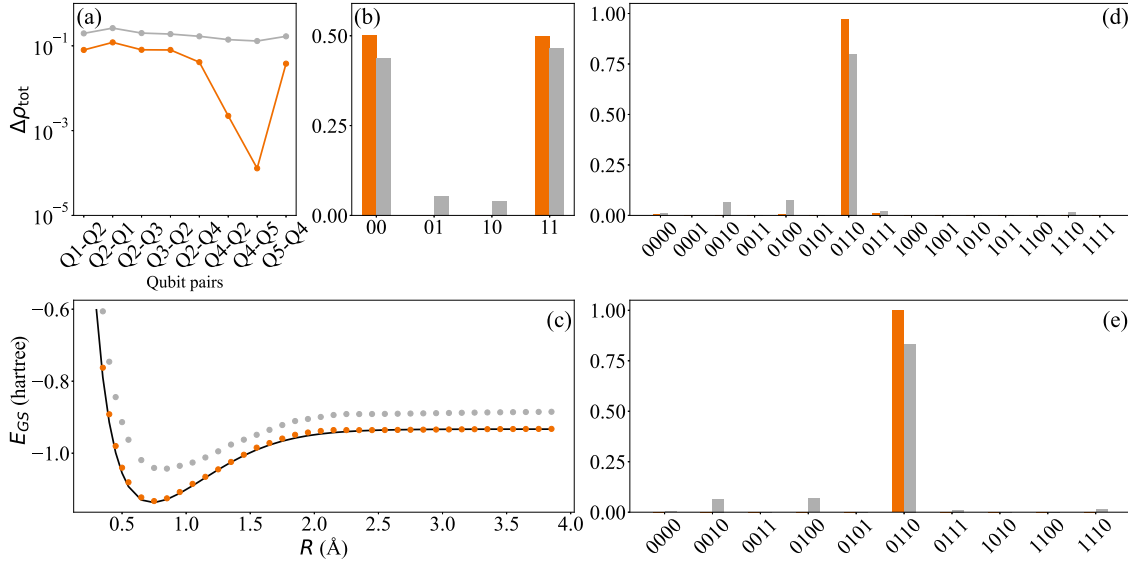


FIG. 4. (a) Total population error  $\Delta\rho_{\text{tot}} = \sum_i |\rho_i^{\text{exact}} - \rho_i^{\text{estimated}}|$  for each qubit pair (the first qubit is the control and the second one is the target in the CNOT), and (b) populations of the pair Q4-Q2, for the Bell state  $|\Phi^+\rangle$  measured using BaLeRO (orange) and count statistics (gray), with  $10^4$  shots. (c)  $H_2$  ground-state energy measured using BaLeRO (orange) and count statistics (gray) using  $10^3$  shots on pair Q1-Q2, compared with the theoretical prediction (black). Populations measured using BaLeRO (orange) and count statistics (gray) in the four qubits system prepared in the state “0110” as output of the Bernstein-Vazirani algorithm in (d) and state preparation through qubit flips in (e), both measured with  $10^4$  shots. All the above demonstrations were performed on IBM Quito.

shots, while with usual readout methods, the readout fidelity is mainly insensitive to the number of repetitions and depends solely on the device’s calibration. It is worth noting that a more in-depth analysis of the QPU setup has the potential to result in more advanced models for the detector response functions, ultimately leading to higher levels of fidelity.

To show the benefits of our approach to the execution of a quantum circuit, we start by considering the application of a single-qubit gate. We choose an arbitrary rotation around the  $y$  axis, i.e., a  $R_y(\theta)$  gate, which results in the final populations  $\rho_g = \cos(\theta/2)^2$  and  $\rho_e = \sin(\theta/2)^2$  when applied to the ground state. Interestingly, our method outperforms the standard readout scheme as it follows more closely the theoretical prediction, as shown for one of the qubits in Fig. 3(c). In Fig. 3(d), we quantify these improvements by displaying the average error on the rotated ground-state population as a function of the number of shots. Our protocol achieves a smaller error than the standard (nonmitigated) case for any number of shots and each qubit. Although the error for the nonmitigated case shows some improvement with an increasing number of shots, saturating around  $10^4$  shots, our approach always offers a dramatic improvement for all qubits.

**Multiqubit use cases and scalability.** A typical quantum algorithm requires to perform two-qubit operations and compute mean values of multiqubit observables. In this section, we show how to employ BaLeRO in such cases and apply it to specific algorithms. Therefore, as the first and simplest extension, let us consider the preparation of the Bell state  $|\Phi^+\rangle = 1/\sqrt{2}(|00\rangle + |11\rangle)$ , which requires the application of a Hadamard gate and a controlled-NOT (CNOT) gate. Thus, we prepare such a state on each directly connected qubit pair, and, as a figure of merit, we calculate the total population error, i.e., deviation from the ideal case, and compare the

one resulting from our readout method with the one from the standard scheme in Fig. 4(a). For each qubit pair, our protocol outperforms the count statistics. As a qualitative example, in Fig. 4(b), we compare the populations of one of the experiments and see how our protocol greatly reduces the populations from the erroneous states, getting closer to the ideal two-qubit state.

In many practical applications, having access to an accurate description of the two-qubit density matrix is crucial. For example, calculating ground-state properties of many-body systems, such as spin chains, requires at most two-body operators. This also applies to simple molecular systems or ferromagnetic models [66], which after “qubitization” have a Hamiltonian with at most two-body operators. As proof of principle, we consider the  $H_2$  molecule, whose ground-state energy can be calculated through a simplified two-qubit system [67,68]. In Fig. 4(c), we show the lower energy extracted using the state preparation ansatz, and Hamiltonian data, of Ref. [36] for  $N_{\text{shots}} = 10^3$ . Again, we see how our method outperforms the nonmitigated one, confirming that the error on the readout is a significant limiting factor in current devices.

Up to two-qubit quantities, the postprocessing algorithm is computationally inexpensive. However, the computational cost increases rapidly, actually exponentially, with the number of qubits, making it unfeasible. For the sake of clarity, for a system with  $N_q$  qubits, Eq. (5) requires handling, at each iteration step of the learning, a multiparameter probability distribution  $\Pr(\rho|\mathbf{x}^{(n)})$  where each variable, i.e., the  $2^{N_q}$  different populations  $\rho_i$ , is sampled in the interval  $[0,1]$ . If each interval is sampled simultaneously with  $n_p$  points, the total probability distribution would require a mesh grid with  $n_p^{2^{N_q}}$  points, albeit the normalization condition reduces the effective number of independent coordinates.

Therefore, it appears quite clear that in the multiqubit scenario our approach is resource intensive and cannot be used as it is, and it requires adaptation. Thus, we follow a heuristic approach, and instead of working with the complete multiparameter probability distribution, we demote all the populations except two, namely,  $\rho_i$  and  $\rho_j$ , to constant estimates  $R_k$ , and define the conditional probability function

$$\Pr(\mathbf{x}|\rho_i, \rho_j) = \rho_i \Pr_i(\mathbf{x}) + \rho_j \Pr_j(\mathbf{x}) + \sum_{k \neq i, j} R_k \Pr_k(\mathbf{x}). \quad (6)$$

Using this, we apply the Bayesian cycle to build a posterior distribution for the population pair in exam, which is then used to compute some new estimates  $R_i$  and  $R_j$ . The algorithm needs to be repeated for each population pair  $(\rho_i, \rho_j)$  and iterated to reach convergence. The convergence criterion can be chosen at will; a simple rule of thumb is to stop the iterations if the change in the posterior probabilities or the obtained populations does not change with respect to the previous iteration by an amount  $\epsilon$ .

To further lighten the computational cost, we reduce the number of parameters  $\rho_i$  included in the optimization procedure. The strategy is to use the initial estimates  $R_k$ , which at the beginning can be the result obtained via the count statistics, to drop states which have a negligible population according to a predefined threshold. In our test we drop from the optimization the states for which we do not get initial counts.

While a highly entangled many-qubit state might still be difficult to reconstruct, we apply our protocol to a quantum algorithm whose theoretical output is a single bitstring, i.e., the Bernstein-Vazirani algorithm [69–71]. In Fig. 4(d), we compare the populations measured using our approach, with parameter region restriction and Bayesian update applied to population pairs, and the count statistics. We apply the Bernstein-Vazirani algorithm on a five-qubit system to obtain the four-qubit string 0110 as an output. Our protocol increases the population of the correct output string, reducing the error from  $\sim 20\%$  to  $\sim 3\%$ . The remaining erroneous populations are mainly due to imperfections in the qubit gates. To confirm it, we prepare the same string, 0110, with a simpler circuit, i.e., by flipping the qubits. The count statistics shows errors

of the same order of magnitude as in the execution of the Bernstein-Vazirani algorithm [Fig. 4(e)], while with BaLeRO we get very close to the expected outcome, reducing the error from  $\sim 16\%$  to  $\sim 0.15\%$ . It is worth mentioning that when measuring multiple qubits simultaneously, the response functions can be affected by a form of correlated noise, i.e., the readout signal of one qubit might be affected by the simultaneous measurement of another. In principle, this correlated noise might be accounted for when calibrating the detector response functions at the cost of a more demanding calibration step. However, in our multiqubit applications, where we performed two-qubit and four-qubit measurements, we have seen a considerable improvement in the readout fidelity, hinting that if the crosstalk is not large, our scheme can correct it even when the fitting functions are built via uncorrelated single-qubit measurements only.

*Conclusions.* We have introduced an efficient readout scheme, BaLeRO, which significantly improves the accuracy of the readout step in quantum computers. The algorithm employs Bayesian inference to build a probability distribution for each qubit-state population based on a reference characterization of the detector response functions, thus including noise and imperfections in the postprocessing of the raw measurement outcomes. Importantly, by design, our Bayesian framework avoids assigning unphysical values and guarantees that the mitigated outcomes are consistent with the experimental data. We tested BaLeRO on two five-qubit quantum computers, demonstrating an accuracy improvement of single- and up to four-qubit readout. It is worth stressing that BaLeRO is not a single-shot postprocessing protocol but a statistical method incorporating the readout noise in the postprocessing, thus improving the reconstruction of the quantum state coherently with the actual measurement.

Finally, while already proving a reduction of the readout error as it is, embedding our scheme within the calibration process of each gate might further boost the performance of NISQ and future devices.

*Acknowledgments.* We acknowledge the use of IBM Quantum services for this work. The views expressed are those of the authors, and do not reflect the official policy or position of IBM or the IBM Quantum team. This work has been partly funded by the Business Finland Co-Innovation Project 40561/31/2020 Quantum Technologies Industrial (QuTI).

- 
- [1] F. Arute, K. Arya, R. Babbush, D. Bacon, J. C. Bardin, R. Barends, R. Biswas, S. Boixo, F. G. S. L. Brandao, D. A. Buell, B. Burkett, Y. Chen, Z. Chen, B. Chiaro, R. Collins, W. Courtney, A. Dunsworth, E. Farhi, B. Foxen, A. Fowler *et al.*, *Nature (London)* **574**, 505 (2019).
- [2] J. Preskill, *Quantum* **2**, 79 (2018).
- [3] A. Kandala, K. Temme, A. D. Córcoles, A. Mezzacapo, J. M. Chow, and J. M. Gambetta, *Nature (London)* **567**, 491 (2019).
- [4] K. Bharti, A. Cervera-Lierta, T. H. Kyaw, T. Haug, S. Alperin-Lea, A. Anand, M. Degroote, H. Heimonen, J. S. Kottmann, T. Menke, W.-K. Mok, S. Sim, L.-C. Kwek, and A. Aspuru-Guzik, *Rev. Mod. Phys.* **94**, 015004 (2022).
- [5] F. Marxer, A. Vepsäläinen, S. W. Jolin, J. Tuorila, A. Landra, C. Ockeloen-Korppi, W. Liu, O. Ahonen, A. Auer, L. Belzane, V. Bergholm, C. F. Chan, K. W. Chan, T. Hiltunen, J. Hotari, E. Hyppä, J. Ikonen, D. Janzso, M. Koistinen, J. Kotilahti *et al.*, *PRX Quantum* **4**, 010314 (2023).
- [6] F.-Y. Li and L.-J. Jin, *Quantum Sci. Technol.* **8**, 045015 (2023).
- [7] F. J. González and R. Coto, *Quantum Sci. Technol.* **7**, 025015 (2022).
- [8] H. P. Bartling, M. H. Abobeih, B. Pingault, M. J. Degen, S. J. H. Loenen, C. E. Bradley, J. Randall, M. Markham, D. J. Twitchen, and T. H. Taminiau, *Phys. Rev. X* **12**, 011048 (2022).
- [9] J. S. Pedernales, F. Cosco, and M. B. Plenio, *Phys. Rev. Lett.* **125**, 090501 (2020).
- [10] Y. You, Z. Ding, and Y. Zhang, *Int. J. Quantum. Inform.* **21**, 2350007 (2023).

- [11] E. Hyypä, S. Kundu, C. F. Chan, A. Gunyhó, J. Hotari, D. Janzso, K. Juliusson, O. Kiuru, J. Kotilahti, A. Landra, W. Liu, F. Marxer, A. Mäkinen, J.-L. Orgiazzi, M. Palma, M. Savvitsky, F. Tosto, J. Tuorila, V. Vadimov, T. Li *et al.*, *Nat. Commun.* **13**, 6895 (2022).
- [12] D. Basilewitsch, F. Cosco, N. L. Gullo, M. Möttönen, T. AlaNissilä, C. P. Koch, and S. Maniscalco, *New J. Phys.* **21**, 093054 (2019).
- [13] M. Abdelhafez, B. Baker, A. Gyenis, P. Mundada, A. A. Houck, D. Schuster, and J. Koch, *Phys. Rev. A* **101**, 022321 (2020).
- [14] T. Bullock, F. Cosco, M. Haddara, S. H. Raja, O. Kerppo, L. Leppäjärvi, O. Siltanen, N. W. Talarico, A. De Pasquale, V. Giovannetti, and S. Maniscalco, *Phys. Rev. A* **98**, 042301 (2018).
- [15] M. Werninghaus, D. J. Egger, F. Roy, S. Machnes, F. K. Wilhelm, and S. Filipp, *npj Quantum Inf.* **7**, 14 (2021).
- [16] S. Endo, S. C. Benjamin, and Y. Li, *Phys. Rev. X* **8**, 031027 (2018).
- [17] S. Endo, Z. Cai, S. C. Benjamin, and X. Yuan, *J. Phys. Soc. Jpn.* **90**, 032001 (2021).
- [18] D. Bultrini, M. H. Gordon, P. Czarnik, A. Arrasmith, M. Cerezo, P. J. Coles, and L. Cincio, *Quantum* **7**, 1034 (2023).
- [19] A. Lowe, M. H. Gordon, P. Czarnik, A. Arrasmith, P. J. Coles, and L. Cincio, *Phys. Rev. Res.* **3**, 033098 (2021).
- [20] Z. Cai, R. Babbush, S. C. Benjamin, S. Endo, W. J. Huggins, Y. Li, J. R. McClean, and T. E. O'Brien, [arXiv:2210.00921](https://arxiv.org/abs/2210.00921).
- [21] A. Strikis, D. Qin, Y. Chen, S. C. Benjamin, and Y. Li, *PRX Quantum* **2**, 040330 (2021).
- [22] J. Kim, B. Oh, Y. Chong, E. Hwang, and D. K. Park, *New J. Phys.* **24**, 073009 (2022).
- [23] R. Takagi, S. Endo, S. Minagawa, and M. Gu, *npj Quantum Inf.* **8**, 114 (2022).
- [24] Y. Kim, C. J. Wood, T. J. Yoder, S. T. Merkel, J. M. Gambetta, K. Temme, and A. Kandala, *Nat. Phys.* **19**, 752 (2023).
- [25] Y. Li and S. C. Benjamin, *Phys. Rev. X* **7**, 021050 (2017).
- [26] K. Temme, S. Bravyi, and J. M. Gambetta, *Phys. Rev. Lett.* **119**, 180509 (2017).
- [27] T. Giurgica-Tiron, Y. Hindy, R. LaRose, A. Mari, and W. J. Zeng, *2020 IEEE International Conference on Quantum Computing and Engineering (QCE)* (IEEE, New York, 2020).
- [28] S. Seo, J. Seong, and J. Bae, [arXiv:2112.10651](https://arxiv.org/abs/2112.10651).
- [29] M. Krebsbach, B. Trauzettel, and A. Calzona, *Phys. Rev. A* **106**, 062436 (2022).
- [30] M. D. Reed, B. M. Maune, R. W. Andrews, M. G. Borselli, K. Eng, M. P. Jura, A. A. Kiselev, T. D. Ladd, S. T. Merkel, I. Milosavljevic, E. J. Pritchett, M. T. Rakher, R. S. Ross, A. E. Schmitz, A. Smith, J. A. Wright, M. F. Gyure, and A. T. Hunter, *Phys. Rev. Lett.* **116**, 110402 (2016).
- [31] T. Walter, P. Kurpiers, S. Gasparinetti, P. Magnard, A. Potočnik, Y. Salathé, M. Pechal, M. Mondal, M. Oppliger, C. Eichler, and A. Wallraff, *Phys. Rev. Appl.* **7**, 054020 (2017).
- [32] P. Harvey-Collard, B. D'Anjou, M. Rudolph, N. T. Jacobson, J. Dominguez, G. A. Ten Eyck, J. R. Wendt, T. Pluym, M. P. Lilly, W. A. Coish, M. Pioro-Ladrière, and M. S. Carroll, *Phys. Rev. X* **8**, 021046 (2018).
- [33] B. D'Anjou and G. Burkard, *Phys. Rev. B* **100**, 245427 (2019).
- [34] J. Heinsoo, C. K. Andersen, A. Remm, S. Krinner, T. Walter, Y. Salathé, S. Gasparinetti, J.-C. Besse, A. Potočnik, A. Wallraff, and C. Eichler, *Phys. Rev. Appl.* **10**, 034040 (2018).
- [35] S. Touzard, A. Kou, N. E. Frattini, V. V. Sivak, S. Puri, A. Grimm, L. Frunzio, S. Shankar, and M. H. Devoret, *Phys. Rev. Lett.* **122**, 080502 (2019).
- [36] M. Urbanek, B. Nachman, and W. A. de Jong, *Phys. Rev. A* **102**, 022427 (2020).
- [37] L. A. Martinez, Y. J. Rosen, and J. L. DuBois, *Phys. Rev. A* **102**, 062426 (2020).
- [38] F. Lecocq, F. Quinlan, K. Cicak, J. Aumentado, S. A. Diddams, and J. D. Teufel, *Nature (London)* **591**, 575 (2021).
- [39] M. R. Geller and M. Sun, *Quantum Sci. Technol.* **6**, 025009 (2021).
- [40] J. Lin, J. J. Wallman, I. Hincks, and R. Laflamme, *Phys. Rev. Res.* **3**, 033285 (2021).
- [41] L. Chen, H.-X. Li, Y. Lu, C. W. Warren, C. J. Križan, S. Kosen, M. Rommel, S. Ahmed, A. Osman, J. Biznárová *et al.*, *npj Quantum Inf.* **9**, 26 (2023).
- [42] S. Maurya, C. N. Mude, W. D. Oliver, B. Lienhard, and S. Tannu, *Proceedings of the 50th Annual International Symposium on Computer Architecture, ISCA '23* (Association for Computing Machinery, New York, 2023).
- [43] S. S. Ivanov, B. T. Torosov, and N. V. Vitanov, *Phys. Rev. Lett.* **129**, 240505 (2022).
- [44] J. Gambetta, W. A. Braff, A. Wallraff, S. M. Girvin, and R. J. Schoelkopf, *Phys. Rev. A* **76**, 012325 (2007).
- [45] F. B. Maciejewski, Z. Zimborás, and M. Oszmaniec, *Quantum* **4**, 257 (2020).
- [46] Y. Chen, M. Farahzad, S. Yoo, and T.-C. Wei, *Phys. Rev. A* **100**, 052315 (2019).
- [47] E. Peters, A. C. Y. Li, and G. N. Perdue, *Phys. Rev. A* **107**, 062426 (2023).
- [48] R. Navarathna, T. Jones, T. Moghaddam, A. Kulikov, R. Beriwal, M. Jerger, P. Pakkiam, and A. Fedorov, *Appl. Phys. Lett.* **119**, 114003 (2021).
- [49] B. Lienhard, A. Vepsäläinen, L. C. Govia, C. R. Hoffer, J. Y. Qiu, D. Ristè, M. Ware, D. Kim, R. Winik, A. Melville, B. Niedzielski, J. Yoder, G. J. Ribeill, T. A. Ohki, H. K. Krovi, T. P. Orlando, S. Gustavsson, and W. D. Oliver, *Phys. Rev. Appl.* **17**, 014024 (2022).
- [50] U. Azad and H. Zhang, Machine learning based discrimination for excited state promoted readout, in *2022 IEEE/ACM 7th Symposium on Edge Computing (SEC)*, Seattle, WA, USA (IEEE, 2022), pp. 362–367, doi:10.1109/SEC54971.2022.00053.
- [51] H. T. Dinani, D. W. Berry, R. Gonzalez, J. R. Maze, and C. Bonato, *Phys. Rev. B* **99**, 125413 (2019).
- [52] R. Puebla, Y. Ban, J. F. Haase, M. B. Plenio, M. Paternostro, and J. Casanova, *Phys. Rev. Appl.* **16**, 024044 (2021).
- [53] B. Teklu, S. Olivares, and M. G. A. Paris, *J. Phys. B: At., Mol. Opt. Phys.* **42**, 035502 (2009).
- [54] S. Paesani, A. A. Gentile, R. Santagati, J. Wang, N. Wiebe, D. P. Tew, J. L. O'Brien, and M. G. Thompson, *Phys. Rev. Lett.* **118**, 100503 (2017).
- [55] K. T. Laverick, I. Guevara, and H. M. Wiseman, *Phys. Rev. A* **104**, 032213 (2021).
- [56] V. Gebhart, A. Smerzi, and L. Pezzè, *Phys. Rev. Appl.* **16**, 014035 (2021).
- [57] S. Duffield, M. Benedetti, and M. Rosenkranz, *Mach. Learn.: Sci. Technol.* **4**, 025007 (2023).
- [58] D. Leibfried, E. Knill, S. Seidelin, J. Britton, R. B. Blakestad, J. Chiaverini, D. B. Hume, W. M. Itano, J. D. Jost, C. Langer *et al.*, *Nature (London)* **438**, 639 (2005).

- [59] J. S. Lundeen, A. Feito, H. Coldenstrodt-Ronge, K. L. Pregnell, C. Silberhorn, T. C. Ralph, J. Eisert, M. B. Plenio, and I. A. Walmsley, *Nat. Phys.* **5**, 27 (2009).
- [60] K. N. Cassemiro, K. Laiho, and C. Silberhorn, *New J. Phys.* **12**, 113052 (2010).
- [61] A. Feito, J. S. Lundeen, H. Coldenstrodt-Ronge, J. Eisert, M. B. Plenio, and I. A. Walmsley, *New J. Phys.* **11**, 093038 (2009).
- [62] A. Blais, A. L. Grimsmo, S. M. Girvin, and A. Wallraff, *Rev. Mod. Phys.* **93**, 025005 (2021).
- [63] See Supplemental Material at <http://link.aps.org/supplemental/10.1103/PhysRevA.108.L060402> for full tables of the QPU parameters as provided by the service provider.
- [64] B. Nachman, M. Urbanek, W. A. de Jong, and C. W. Bauer, *npj Quantum Inf.* **6**, 84 (2020).
- [65] R. Hicks, C. W. Bauer, and B. Nachman, *Phys. Rev. A* **103**, 022407 (2021).
- [66] R. N. Tazhigulov, S.-N. Sun, R. Haghshenas, H. Zhai, A. T. Tan, N. C. Rubin, R. Babbush, A. J. Minnich, and G. K.-L. Chan, *PRX Quantum* **3**, 040318 (2022).
- [67] P. J. J. O'Malley, R. Babbush, I. D. Kivlichan, J. Romero, J. R. McClean, R. Barends, J. Kelly, P. Roushan, A. Tranter, N. Ding, B. Campbell, Y. Chen, Z. Chen, B. Chiaro, A. Dunsworth, A. G. Fowler, E. Jeffrey, E. Lucero, A. Megrant, J. Y. Mutus *et al.*, *Phys. Rev. X* **6**, 031007 (2016).
- [68] M. Ganzhorn, D. Egger, P. Barkoutsos, P. Ollitrault, G. Salis, N. Moll, M. Roth, A. Fuhrer, P. Mueller, S. Woerner, I. Tavernelli, and S. Filipp, *Phys. Rev. Appl.* **11**, 044092 (2019).
- [69] E. Bernstein and U. Vazirani, *SIAM J. Comput.* **26**, 1411 (1997).
- [70] D. R. Simon, *SIAM J. Comput.* **26**, 1474 (1997).
- [71] B. Pokharel and D. A. Lidar, *Phys. Rev. Lett.* **130**, 210602 (2023).